Journal of Physics: Conference Series **656** (2015) 012027 doi:10.1088/1742-6596/656/1/012027

Modeling and experimental analysis of acoustic cavitation bubbles for Burst Wave Lithotripsy

Kazuki Maeda[1], Wayne Kreider[2], Adam Maxwell[2,3], Bryan Cunitz[2], Tim Colonius[1], and Michael Bailey[2,3]

[1]Devision of Engineering and Applied Science, 1200 E California Blvd, Pasadena, California 91125

[2]Center for Industrial and Medical Ultrasound, Applied Physics Laboratory, University of Washington, 1013 NE 40th St, Seattle, WA 98105.

[3]Department of Urology, University of Washington School of Medicine, 1959 NE Pacific St, Seattle, WA 98195

E-mail: maeda@caltech.edu

Abstract. Cavitation bubbles initiated by focused ultrasound waves are investigated through experiments and modeling. Pulses of focused ultrasound with a frequency of 335 kHz and a peak negative pressure of 8 MPa is generated in a water tank by a piezoelectric transducer to initiate cavitation. The pressure field is modeled by solving the Euler equations and used to simulate single bubble oscillation. The characteristics of cavitation bubbles observed by high-speed photography qualitatively agree with the simulation results. Finally, bubble clouds are captured using acoustic B-mode imaging that works synchronized with high-speed photography.

Burst Wave Lithotripsy (BWL) is a newly proposed non-invasive medical procedure to fragment kidney stones by focused ultrasound pulses of amplitude $O(1)$ MPa[1]. BWL is a potential alternative to Shock Wave Lithotripsy (SWL), a widely used procedure in clinical treatments that typically utilizes shock waves of $O(10)$ MPa for stone fragmentation; BWL enables comminution of stones into smaller fragmentations with lower peak pressure[1]. In both procedures, acoustic cavitation can be initiated during the passage of the tensile parts of the pressure wave of amplitude $O(1)$ MPa inside human body. Cavitation activity is important in such treatments because it can both erode kidney stones and cause tissue injury[2]. Because bubbles strongly interact with the incident sound field, cavitation can also be counterproductive by shielding the stone from the incident waves[3]. However, the fundamental physics of cavitation bubbles in strong interaction with the focused ultrasound field has not been fully studied in detail.

We report on combined modeling and experimental study of cavitation bubbles that are initiated by BWL-type ultrasound pulses in an open water tank. We generate waves using a piezoelectric transducer that has been used to break stones in both in vitro and in vivo environments[1]. In the modeling, we analytically emulate the transducer and simulate the sound field generated by the transducer in detail by solving the Euler equations. In the experiment, we observe the evolution of the cavitation bubble cloud using high-speed photography combined with B-mode acoustic imaging. The captured bubble clouds are in a qualitative agreement with the radial evolution of single spherical bubble calculated using Keller-Miksis equation combined with the pressure field from the simulations. Finally, through synchronization with the high-

speed photography, we confirmed the potential of B-mode ultrasound imaging to effectively characterize bubble activity. The agreement among the modeling and the experimental measurements would lead to further understanding of the cavitation bubbles for BWL.

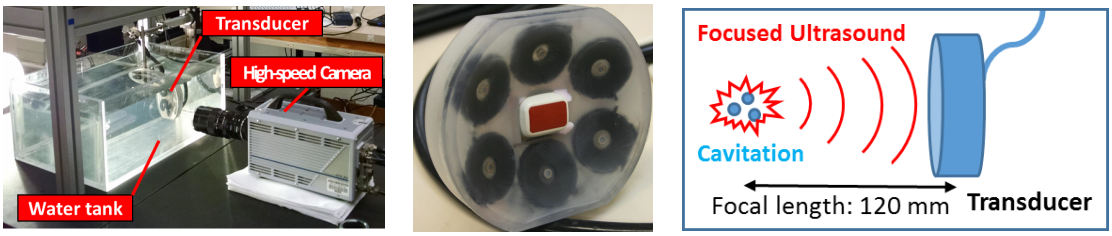

(a) Experimental setup (b) Transducer (c) Schematic

Figure 1. The images and the schematic of the experimental setup.

Figure 1 shows the experimental setup used for the generation and observation of cavitation bubbles. The piezoelectric transducer shown in figure 1b has 120 mm focal length and generates waves of frequency 335 kHz. An imaging probe (ATL HDI P4-2) is mounted in the center of the transducer. The high-speed camera (Model APX-RS camera, Photron USA, Inc., San Diego, CA) is triggered to captures images around the focal region of the transducer from the side of the tank (figure 1c) at 20,000 fps, when the waves arrive at the region. Tap water which was filtered and degassed to 65% O_2 level was used. The BWL pulses are characterized by the pulse repetition frequency (PRF), wave cycles per pulse (N_c), the total number of pulses (N_p) and maximum focal pressure P_f. In the present study, we use sinusoidal form of waves characterized by PRF= 200 Hz, $N_c = 10$, $N_p = 100$ and $P_f = 8$ MPa.

Figure 2 shows the pressure field at instances during the passage of the 10 cycles of left-going wave sent from the model transducer. The transducer is modeled as a spherical cup of 100 mm with its center located at the origin. The water is modeled as an inviscid fluid that follows stiffened gas equation of state. Acoustic monopoles and dipoles are distributed on the transducer surface such left-going waves of designated amplitude are generated. The simulation algorithm[4] uses a high-order accurate finite-volume weighted essentially non-oscillatory (WENO) reconstruction, to obtain the primitive flow variables at the cell-boundaries, and a Harten-Lax-van Leer-Contact (HLLC) approximate Riemann solver, to compute the

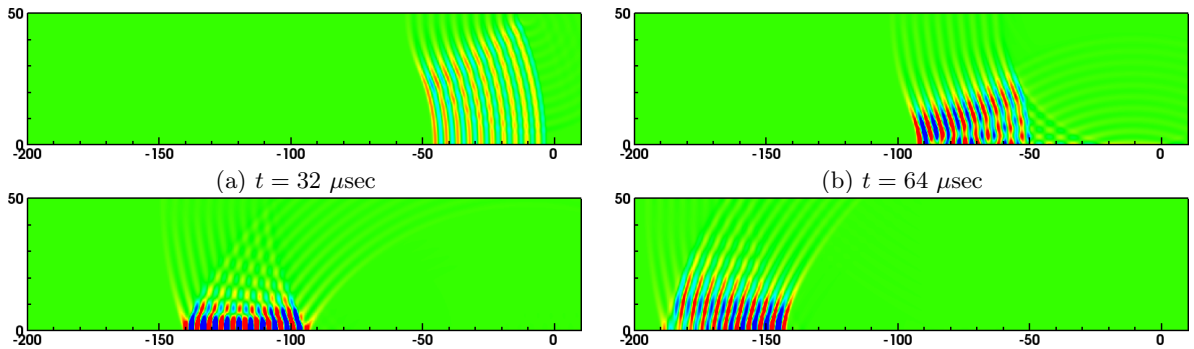

(a) $t = 32$ μsec (b) $t = 64$ μsec

(c) $t = 96$ μsec (d) $t = 128$ μsec

Figure 2. The flooded pressure contour of the wave sent from the model transducer along the upper half of a plane of symmetry of the 2D cylindrical domain. The red and blue color denote high and low pressure regions, respectively. The number of grid points used in the simulation is $[N_x,\ N_y] = 1250 \times 300$. The unit of the axis labels is mm.

resulting fluxes. Time marching is handled by a total-variation-diminishing Runge-Kutta (TVD-RK) time-stepper.

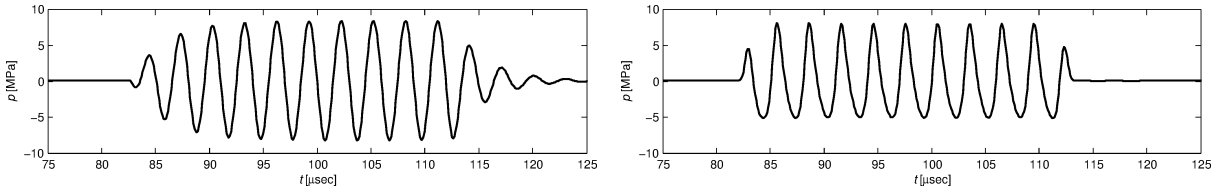

(a) Linear model (b) DNS

Figure 3. The focal pressure evolution of the waves sent from the transducer.

Figure 3 shows the focal pressure obtained from a linear transducer model that includes ring-up/ring-down effects, and that of the simulation. Though the simulated wave-form presents slight non-linear distortion and does not include the ring-up/ring-down effects, the values of peak maximum pressure as well as the qualitative wave forms agree.

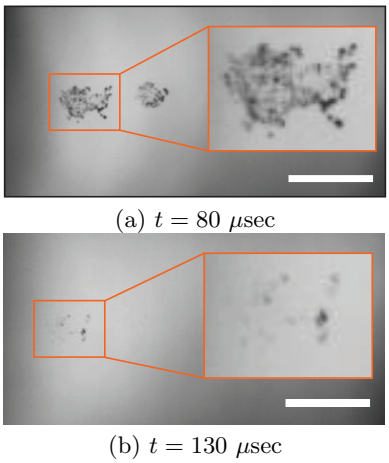

(a) $t = 80$ μsec

(b) $t = 130$ μsec

Figure 4. High-speed images taken at $t = 80$ μsec and 130 μsec during the 3rd pulse. The scale bars denote 5 mm.

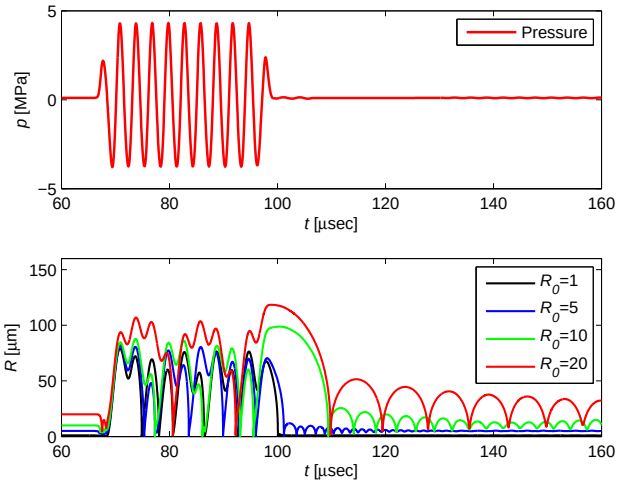

Figure 5. Simulated pressure evolution at $(x, y) = (-98, 0)$ and the corresponding radial evolution of isolated bubbles responding to the focal pressure with various initial radii.

Figure 4 shows the representative images of cavitation bubbles captured by the high-speed camera at $t = 80$ μsec and 130 μsec during the 3rd pulse, where $t = 0$ is the moment when the transducer was triggered to generate the pulse. The location of the center of the images correspond to (-98, 0) in the images of figure 2, thus 98 mm distant from the center of the transducer. At $t = 80$ μsec, we see two bubble clouds as large as 3 mm. In the magnified inset, the presence of individual bubble can be confirmed in the leftmost cloud. At $t = 130$ μsec, the clouds disappear and a few bubbles are discretely observed. We note that this tendency of the shrinkage of the cloud was confirmed in the images from different pulses, though the locations and the sizes of the bubble clouds were not consistent.

Figure 5 shows the pressure evolution at (-98, 0) obtained using the simulated pressure field and the corresponding radial evolution of pre-existing bubble nuclei with typical size, that are computed using the Keller-Miksis equation[5]. Around 80 μsec, bubbles oscillate to reach the maximum radius around 100 μm, while at $t = 130$ μsec, only bubbles with large initial radius (10 μm and 20 μm) remain and collapse and rebound to radii less than 50 μm. Bubbles with

initial radius 1 and 5 μm are immediately damped after the passage of the wave, due to strong acoustic radiations. Thus at $t = 130$ μm we would assume to see fewer number of bubbles of smaller size. This assumption corresponds to the observation in figure 4.

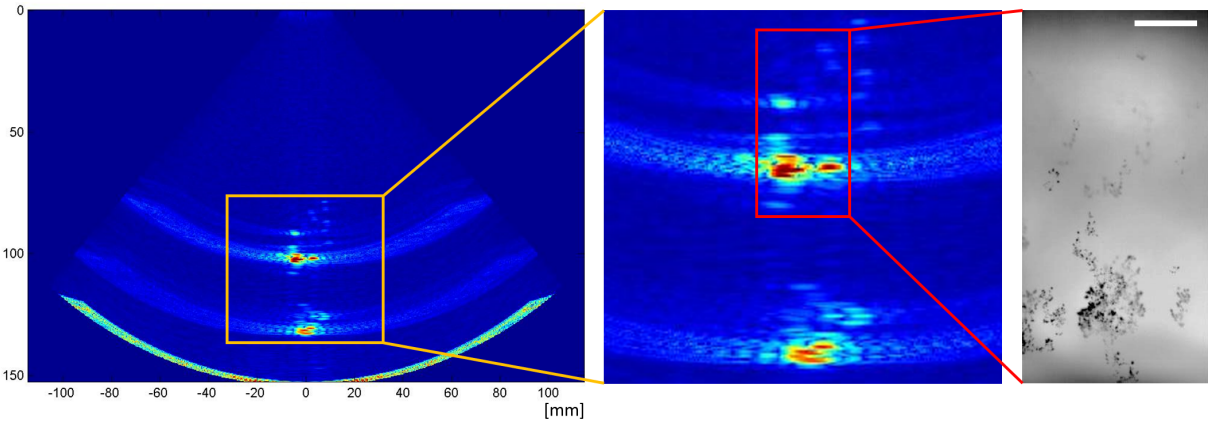

Figure 6. The images of cavitation bubbles taken by synchronized B-mode acoustic imaging (the left and middle images) and high-speed photography (the right image) at $t = 100$ μsec. The waves propagate from the top to the bottom of the images. The scale bar in the photographic image denotes 5 mm.

Finally, figure 6 shows representative images of cavitation bubbles obtained using synchronized B-mode imaging and high-speed photography. B-mode images were captured at 400 frames per BWL-pulse, using the imaging probe with a Verasonics ultrasound engine (Kirkland, WA, USA). Because the open water tank is devoid of scatterers other than bubbles, the intense regions in reconstructed images should correspond to bubbles. Though the fps of the imaging pulse is much lower than that of high-speed photography, the size and location of bubble clouds in the B-mode image agrees well with those of the high-speed photography, suggesting its potential for detecting bubble activity during treatment.

In conclusion, we have confirmed the qualitative agreement between modeling and experiments in terms of the radial evolution of isolated bubbles responding to focal pressure field simulated by solving the Euler equations. B-mode imaging and high-speed photography were successfully synchronized during the pulses. For further quantitative analysis of the acoustic cavitation, we plan to extend the present study by modeling bubble clouds taking inter-bubble interactions[6] into account and by measuring the pressure field simultaneously with higher-speed photography to capture the dynamics of the cloud in detail.

Acknowledgment

The authors thank Dr. Julianna Simon and Barbrina Dunmire for support in the experimental measurements, Prof. Jonathan Freund, Dr. Pooya Movahed, Dr. Vedran Coralic, and Jomela Meng for helpful discussions. The work was supported by the National Institutes of Health under grant 2PO1-DK043881.

References

[1] Maxwell A D, Cunitz B W, Kreider W, Sapozhnikov O A, Hsi R S, Harper J D, Bailey M R and Sorensen M D 2015 *J Urol* **193** 338–344
[2] Maxwell A D, Cain C A, Duryea A P, Yuan L and Gurm H S 2009 *Ultrasound Med. Biol.* **12** 1982–1994
[3] Tanguay M 2004 Ph.D. thesis California Institute of Technology
[4] Coralic V and Colonius T 2014 *J. Comput. Phys.* **274** 95–121
[5] Keller J B and Miksis M 1980 *J. Acoust. Soc. Am.* **68** 628–633
[6] Fuster D and Colonius T 2011 *J. Fluid Mech.* **688** 352–389 ISSN 0022-1120